SCRS/2021/058 Collect. Vol. Sci. Pap. ICCAT, 78(2): 231-252 (2021)

INDEX OF ABUNDANCE OF JUVENILE BIGEYE TUNA IN THE ATLANTIC OCEAN DERIVED FROM ECHOSOUNDER BUOYS (2010-2020)

J. Santiago[1], *J. Uranga*[1], *I. Quincoces*[1],
M. Grande[1], *H. Murua*[2], *G. Merino*[1], *I. Zudaire, A. Urtizberea*[1], *G. Boyra*[1]

SUMMARY

The collaboration with the Spanish vessel-owners associations and the buoy-providers companies, has made it possible the recovery of the information recorded by the satellite linked GPS tracking echosounder buoys used by the Spanish tropical tuna purse seiners and associated fleet in the Atlantic since 2010. These instrumental buoys inform fishers remotely in real-time about the accurate geolocation of the FAD and the presence and abundance of fish aggregations underneath them. Echosounder buoys have the potential of being a privileged observation platform to evaluate abundances of tunas and accompanying species using catch-independent data. Current echosounder buoys provide a single acoustic value without discriminating species or size composition of the fish underneath the FAD. Therefore, it has been necessary to combine the echosounder buoys data with fishery data, species composition and average size, to obtain a specific indicator. This paper presents a novel index of abundance of juvenile bigeye tuna in the Atlantic Ocean derived from echosounder buoys for the period 2010-2020.

RÉSUMÉ

La collaboration avec les associations d'armateurs espagnols et les fournisseurs de bouées a permis de récupérer les informations enregistrées par les bouées associées à un échosondeur de suivi GPS par satellite utilisées par les senneurs espagnols ciblant les thonidés tropicaux et la flottille associée dans l'Atlantique depuis 2010. Ces bouées instrumentales informent les pêcheurs à distance et en temps réel de la géolocalisation précise du DCP ainsi que de la présence et de l'abondance des concentrations de poissons en dessous. Les bouées associées à un échosondeur peuvent constituer une plateforme d'observation privilégiée pour évaluer l'abondance des thonidés et des espèces qui les accompagnent à partir de données indépendantes des captures. Les bouées associées à un échosondeur actuelles fournissent une seule valeur acoustique sans distinguer l'espèce ou la composition par taille du poisson sous le DCP. Il a donc été nécessaire de combiner les données des bouées associées à un échosondeur avec les données des pêcheries, la composition des espèces et la taille moyenne, afin d'obtenir un indicateur spécifique. Ce document présente un nouvel indice d'abondance des juvéniles de thon obèse dans l'océan Atlantique, dérivé à partir des bouées associées à un échosondeur pour la période 2010-2020.

RESUMEN

La colaboración con las asociaciones de armadores españoles y las compañías proveedoras de boyas ha hecho posible la recuperación de la información grabada por el GPS por satélite que rastrea las boyas ecosonda utilizadas por los cerqueros españoles y la flota asociada que se dirigen a los túnidos tropicales del Atlántico desde 2010. Estas boyas instrumentales informan a los pescadores de forma remota y en tiempo real acerca de la geolocalización de los DCP y de la presencia y abundancia de las agregaciones de peces bajo ellos. Las boyas ecosonda tienen el potencial de ser una plataforma privilegiada de observación para evaluar la abundancia de túnidos y las especies que los acompañan utilizando datos independientes de la captura. Las actuales boyas ecosonda proporcionan un único valor acústico sin discriminar la composición por especies o por tallas de los peces bajo el DCP. Por lo tanto, ha sido necesario combinar los datos de las boyas ecosonda con los datos pesqueros, la composición por especies y la talla media para obtener un indicador específico. Este documento presenta un nuevo índice de abundancia de patudo juvenil en el océano Atlántico derivado de las boyas ecosonda para el periodo 2010-2020.

KEYWORDS

Acoustics, Echosounder buoys, Abundance index, Bigeye tuna, FADs

[1] AZTI, Marine Research, Basque Research and Technology Alliance (BRTA). Txatxarramendi ugartea z/g, 48395 Sukarrieta - Bizkaia, Spain
[2] ISSF, International Seafood Sustainability Foundation, Washington DC – USA

1. Introduction

Fishery stock assessment models are demographic analyses designed to determine the effects of fishing on fish populations and to evaluate the potential consequences of alternative harvest policies (Methot & Wetzel, 2012). Quantification of fish populations is the central part of any fish stock assessment, and it is commonly the most difficult task. This is even more complicated in the case of highly migratory fish stocks, such as tuna, were conventional fishery-independent surveys are in general not practicable. And, in the absence of fishery-independent information, most of the abundance indices used in fish stock assessments are derived from estimates of Catch per Unit Effort (CPUE), the number or biomass of fish caught as a function of effort (Quinn & Deriso, 1999).

Relative abundance indices based on CPUE data are notoriously problematic (Maunder *et al.*, 2006), as catch data is usually biased by fishing effort, coverage, and other limiting factors of fishery data. The primary assumption behind a CPUE-based abundance index is that changes in the index are assumed to be proportional to changes in the actual stock abundance (Maunder & Punt, 2004), being catchability (q) -the portion of the stock captured by one unit of effort - the coefficient of proportionality. One of the associated difficulties is that q is rarely constant and depends on several different components, such as those related to changes in the fishing efficiency and dynamics of the fleet.

Tropical tuna purse seining is one of such fisheries where both factors, fishing efficiency and dynamics of the fleet, are evolving very rapidly due to the fast technological development (Torres-Irineo *et al.*, 2014) and the sharp increase of the use of Fish Aggregating Devices (FADs) (Scott & Lopez, 2014). This fact makes it difficult to obtain reliable CPUE indices for tropical tunas from purse fisheries fishing under drifting FADs. Recent initiatives such as the EU funded projects RECOLAPE, CECOFAD-1 and CECOFAD-2 are focusing on the understanding of the use of FADs in tropical purse seine tuna fisheries and to try to provide reliable estimates of abundance indices (Gaertner *et al.*, 2016). And science-industry collaboration in the context of these and other projects is clearly improving the understanding of the FAD use but also the availability of data with great potential for improving CPUE indices and for developing novel abundance indicators.

The collaboration with the Spanish vessel-owners associations (ANABAC and OPAGAC) and the buoy-providers companies (Marine Instruments, Satlink and Zunibal), has made it possible the recovery of the information recorded by the satellite tracking echosounder buoys used by the Spanish tropical tuna purse seiners and associated fleet in the Atlantic for the period 2010-2020. These instrumental buoys inform fishers remotely in near real-time about the accurate geolocation of the FAD and the presence and abundance of tuna aggregations underneath them. Apart from its unquestionable impact in the conception of a reliable CPUE index from the purse seine tropical tuna fisheries fishing on FADs, echosounder buoys have also the potential of being a privileged observation platform to evaluate abundances of tunas and accompanying species using catch-independent data (Dagorn *et al.*, 2006; Lopez *et al.*, 2014; Santiago *et al.*, 2016, 2019).

Current echosounder buoys provide a single acoustic value without discriminating species or size composition of the fish underneath the FAD. Therefore, it has been necessary to combine the echosounder buoys data with fishery data, species composition and average size, to obtain a specific indicator. This paper presents a novel index of abundance of juvenile bigeye tuna in the Atlantic Ocean derived from echosounder buoys for the period 2010-2020. Equivalent indices were developed in 2019 for the Atlantic and Indian Ocean yellowfin tuna stocks and for the Indian Ocean skipjack in 2020 following the same methodology described here (Santiago *et al.*, 2019, 2020a,b).

2. Material and methods

2.1 The acoustic data

Acoustic data from echosounder buoys used in this analysis have been provided by the company Satlink. This type of buoy is equipped with a sounder, which operates at a frequency of 190.5 kHz with a power of 100 W. The range extends from 3 to 115 m, with a transducer blanking zone running from 0 to 3 m. At an angle of 32°, the cone of observation under the buoy has a diameter of 78.6 m at a depth of 115 m. The echosounder provides acoustic information in 10 different vertical layers, each with a resolution of 11.2 m. During the period analysed three different buoy models have been used by the fleet: DS+, DSL+ and ISL+. These three buoy models work with similar beam angle, frequency and power, and with the above mention vertical stratification. DSL+ and DS+ obtain three acoustic records per day, i.e. before dawn, at dawn and after dawn in the default mode. ISL+ has the capacity to sample along the day each 15 minutes, transmitting the signal if the value recorded for a 24 hours period is larger than the previous record.

The fishing companies belonging to ANABAC and OPAGAC that have provided acoustic information from their echosounder buoys were: Albacora SA, Atunera Sant Yago SA, Atunsa, Calvopesca El Salvador SA de CV, Cantabrica de Tunidos SAU, Icube Tuna Fisheries NV, Inpesca Fishing Belize Ltd, Integral Fishing Service INC, Intertuna, NV, Overseas Tuna Company NV and Pevasa. This adds up to a total of 27 purse seine vessels from 7 different flags (Belize, Cabo Verde, Curacao, El Salvador, Spain, Guatemala and Panama) operating in the ICCAT convention area.

The database of acoustic information of the Atlantic Ocean from Satlink buoys comprises around 15 million of records from over 40,000 buoys for the period from January 2010 to December 2020. The information on buoy positions and acoustic information is received in two different data-sets with the following fields:

- Data-set on buoy positions
  - *Date*: Date of the last position of the day
  - *Time*: Hour (GMT)
  - *Buoy code*: Unique identification number of the buoy, given by the model code (D+, DS+, DL+, DSL+, ISL+, ISD+ followed by 5-6 digits.
  - *Latitude:* Latitude of the last position of the day (in decimals)
  - *Longitude*: Longitude of the last position of the day (in decimals)
  - *Velocity*: v calculated from the distance/time between the last position of the day and the last position of the previous day.
  - *Notes:* Empty column

- Data-set on acoustic records
  - *Name*: Unique identification number of the buoy, given by the model code (D+, DS+, DL+, DSL+, ISL+, ISD+ followed by 5-6 digits.
  - *OwnerName*: Name of the buoy owner assigned to a unique purse seine vessel
  - *MD*: Message descriptor (160, 161 and 162 for position data, without sounder data, and 163, 168, 169 and 174 for sounder data)
  - *StoredTime*: Date (dd/mm/yyyy) and hour (H:MM) of the echosounder record
  - *Latitude, Longitude*: Not provided (this information is provided in the position data-set)
  - *Bat*: Not provided. (Charge level (in percentage). Except for the D+ and DS+ in voltage)
  - *Temp*: Temperature (Not provided)
  - *Speed*: Speed in knots (Not provided)
  - *Drift*: bearing in degrees (Not provided)
  - *Layer1-Layer10*: Depth observation range extends from 3 to 115 m, which is split in ten homogeneous layers, each with a resolution of 11.2 m. The buoy has also a blanking zone (a data exclusion zone to eliminate the near-field effect of the transducer between 0 and 3 m. 32 pings are sent from the transducer and an average of the backscattered acoustic response is computed and stored in the memory of the buoy. Manufacturer´s method converts raw acoustic backscatter into biomass in tons, using a depth layer echo-integration procedure based exclusively on an algorithm based on the TS and weight of skipjack tuna.
  - *Sum*: Sum of the biomass estimated at each layer
  - *Max*: Maximum biomass estimated at any layer
  - *Mag1, Mag3, Mag5 and Mag7*: Magnitudes corresponding to the counts of detected targets according to the TS of the detection peak.

2.2 From acoustic data to a species-specific abundance indicator

To calculate the biomass aggregated under a FAD from the acoustic signal, Satlink uses the density of one species, skipjack, to provide the biomass in tons, biomass data from Satlink was converted to decibels reversing their formula for the biomass computation. Then we recomputed biomass using standard abundance estimations equations (Simmonds & MacLennan, 2005):

$$Biomass_i = \frac{s_V \cdot Vol \cdot p_i}{\sum_i \sigma_i \cdot p_i}$$

where *Vol* is the sampled volume and p_i and σ_i are the proportion and linearized target strength of each species *i* respectively. Species proportions in weight were extracted from the logbooks of the fleet associated to OPAGAC (19 vessels) for each 1ºx1º and month stratum, as explained below. Mean fish lengths (L_i) used for skipjack (SKJ), bigeye (BET) and yellowfin (YFT) were obtained from ICCAT T2CS - catch-at-size, and weights were obtained using weight-length relationships (ICCAT conversion factors). Then, the following TS-length relationships were used to obtain linearized target strength per kilogram:

$$\sigma_i = \frac{10^{(20\log(L_i)+b_{20,i})/10}}{w_i}$$

Where w_i is the mean weight of each species. Given that each brand uses different operating frequencies, we used different b20 values for each. For Satlink, the b20 values were obtained from (Boyra *et al.*, 2018) for SKJ and (Oshima, 2008) for YFT and BET.

Since all acoustic data is not covered with a corresponding species distribution data from the logbook data, buoy distributions and species composition at the same 1ºx1º grid, year and month were filtered and assigned. The rest of the acoustic observations were excluded for this analysis.

2.3 Acoustic data cleaning and filtering

Data cleaning included the removal of records without acoustic information (records with only position, speed and velocity), outliers (invalid, impossible or extreme values) related to bad geolocation, time, or other general variables. And aside of the regular exclusions due to this type of inconsistencies, the following considerations were also taken into account for accepting the data for the standardization analysis:

- *Vertical boundary between tuna and non-tuna species:* acoustic information from the shallower layers, <25m, was not considered for the analysis. According to (Lopez *et al.*, 2017; Robert *et al.*, 2013), the vertical boundary between non-tuna species and tunas can be considered at about 25 m. Excluding the first layers, we try to eliminate noise from the non-tuna species associated to the FAD.
- *Bottom depth*: Using high resolution bathymetry data (British Oceanographic Data Centre, UK, www.gebco.net), acoustic records from buoys located in areas with a bottom depth shallower than 200 m were excluded. The rational of this exclusion is not to incorporate acoustic records of FADs that have drifted to coastal areas were tunas are less likely to be present.
- *Acoustic measurements at sea*: Buoys are normally turned on before deployment, so some records may correspond to onboard buoys. To deal with this issue we developed a Random Forest (RF) model (Orue *et al.*, 2019) to classify the buoys at sea and onboard using information from Zunibal buoys. These buoys have the capability to identify between positions at sea or onboard, using a conductivity sensor. The sensor measures the current between two electrodes and through a simple algorithm it determines whether the Zunibal buoy is inside or outside the water. Those records classified as onboard were excluded.
- *Time of the day:* Only those samples obtained around sunrise, between 4 a.m. and 8 a.m., were considered for the analysis. These samples are supposed to capture the echosounder biomass signals that better represents the abundance of fish under the FADs, as this is the time when tuna is observed to be more closely aggregated around the FADs (Brill *et al.*, 1999; Josse *et al.*, 1998; Moreno *et al.*, 2007). For the specific case of comparing the acoustic data with abundance it is important that the echosounder measurements are received when the signal is more representative of the biomass around the FAD model (Orue *et al.*, 2019).
- *Days since deployment:* The objective of this selection criterium was to consider those acoustic records that were more likely associated to FAD trajectory, termed "virgin segments".
  A virgin segment is defined as the segment of a buoy trajectory whose associated FAD likely represents a new deployment which has been potentially colonized by tuna and not already fished. Orue *et al.*, (2019) concluded that tuna seemed to arrive at FADs in 13.5±8.4 days and, thus, we consider as virgin segments (i.e. when tuna has aggregated to FAD) those segments of trajectories from 20-35 days at sea.
  In order to identify and separate those segments and their acoustic samples, the overall trajectories of the entire life-time of each buoy were fractioned in smaller sequences corresponding to periods where they could have been attached to different FADs. A new sequence of a buoy was considered to occur, and hence an attachment to a new FAD, when the difference between two consecutive observations of the same buoy was larger than 30 days. Each sequence was assigned with a "new trajectory code" that included the code of the buoy plus the consecutive number of the sequence of each buoy. A deployment/redeployment of a buoy was considered to occur when the "new trajectory code" appears for the first time in the database.

Sequences with less than 30 observations were excluded from the analysis. Sequences having a time difference between any of the consecutive observations longer than 4 days during the first 35 days were also excluded.

Figure 1 shows a diagram with an example of “virgin” segments used for the calculation of the BAI index.

– *Detection threshold:* Acoustic records equal or less than 0,1 tonnes were considered zeros. This is a conservative preliminary value since further validation is needed.

2.4 The BAI index: Buoy-derived Abundance Index

The estimator of abundance BAI was defined as the 0.9 quantile of the integrated acoustic energy observations in each of the "virgin" sequences. A high quantile was chosen because the large values are considered to be likely produced by tuna (in opposition to plankton or bycatch species). This assumption is followed by all the buoy brands in the market, which use the maximum value as the summary of each time interval. In our case we selected a high quantile instead of the maximum to try to provide a more robust estimator by avoiding eventual outlier values. We did this to avoid taking into account the expected lowest values that might appear after eventual hauls occurring along the sequence. The total number of “virgin” sequences analysed, and hence the number of observations in the model, rose to 35,141, of which 34,142 (97.16%) were positives.

2.5 Covariates

Covariates included year-quarter (yyqq), and 5°x5º ICCAT areas fitted as categorical variables. Other variables used in the standardization process included velocity of the buoy, FAD densities and a set of environmental variables. They were chosen for potential effects on the horizontal-vertical distribution of tunas and their association to FADs (FAD density, mixed layer height, sea surface temperature, chlorophyll concentration and detected fronts in sea surface temperature and chlorophyll daily datasets computed with Belkin and O’Reilly method) or on the quality of the echosounder measurements (buoy velocity). These variables were incorporated in the model as continuous variables.

A proxy of 1ºx1º and monthly FAD densities were calculated as the average number of buoys over each month by summing up the total number of active buoys recorded per day over the entire month and dividing by the total number of days.

The environmental variables evaluated in the model were:

- *Ocean mixed layer thickness:* defined as the depth where the density increase compared to density at 10 m depth corresponds to a temperature decrease of 0.2°C in local surface conditions (θ10m, S10m, P0= 0 db, surface pressure).
- *Chlorophyll:* Mass concentration of chlorophyll a in sea water (depth = 0).
- *Sea Surface Temperature* (SST)
- *SST and Chlorophyll fronts:* Oceanographic front detection was performed using the “grec” package for R for each daily dataset, that provides algorithms for detection of spatial patterns from oceanographic data using image processing methods based on Gradient Recognition (Belkin & O’Reilly, 2009).

Figure 2 shows an example of one month of data, January 2010, of buoy trajectories, density of buoys by 1ºx1º rectangles and environmental variables incorporated in the GLM analysis.

2.6 The model

The model we propose is based in an assumption very similar to the fundamental relationship among CPUE and abundance widely used in quantitative fisheries analysis. In our case we built the index based on the assumption that the signal from the echosounder is proportional to the abundance of fish.

$$BAI_t = \varphi \, . B_t$$

where BAI_t is the Buoy-derived Abundance Index and B_t is the abundance in time t (Santiago *et al.,* 2016).

Although it would appear to be obvious, there is not plenty of literature on the relationship between acoustic indicators and fishing performance. It is assumed that acoustic echo integration is a linear process, i.e., proportional to the number of targets (Simmonds & MacLennan, 2005) and has been experimentally proven to be correct with some limitations (Foote, 1983; Røttingen, 1976). Therefore, acoustic data (echo integration) is commonly taken as an estimator of abundance and is thoroughly applied to provide acoustic estimation of abundance of many pelagic species (e.g., Hampton, 1996; ICES, 2015; Massé, Uriarte, Angélico, & Carrera, 2018).

As with the catchability, the coefficient of proportionality φ is not constant for many reasons. In order to ensure that φ can be assumed to be constant (i.e. to control the effects other than those caused by changes in the abundance of the population) a standardization analysis should be performed aiming to remove factors other than changes in abundance of the population. This can be performed standardizing nominal measurements of the echosounders using a Generalized Linear Mixed Modelling approach.

Considering the low proportion of zero values (2.84%) the delta lognormal approach (Lo *et al.*, 1992) was not considered. GLMM (log-normal error structured model) was applied to standardize the acoustic observations. A stepwise regression was applied to the model with all the explanatory variables and interactions in order to determine those that significantly contributed to explain the deviance of the model. For this, deviance analysis tables were created for the positive acoustic records. Final selection of explanatory factors was conditional to: a) the relative percentage of deviance explained by adding the factor in evaluation (normally factors that explained more than 5% were selected), and b) The Chi-square ($\chi 2$) significance test. Those factors that explained less than 5% of the variability of the model were not considered.

Interactions of the temporal component (year-quarter) with the rest of the variables were also evaluated. If an interaction was statically significant, it was then considered as a random interaction(s) within the final model (Maunder & Punt, 2004).

Lastly, the selection of the final mixed model was based on the Akaike's Information Criterion (AIC), the Bayesian Information Criterion (BIC), and a Chi-square ($\chi 2$) test of the difference between the log-likelihood statistic of different model formulations. The year-quarter effect least square means (LSmeans) use a weighted factor of the proportional observed margins in the input data to account for the non-balance characteristics of the data. The LSMeans were bias corrected for the logarithm transformation algorithms using Lo *et al.* (1992). All analyses were done using the lme4 package for R (Bates *et al.*, 2015).

3. Results

A total of 15 million of records from more than 40,000 buoys for the period from January 2010 to December 2020 were integrated into 34,142 observations for the GLM analysis. Each observation was calculated as the 90% percentile of a "virgin" segment of buoy trajectories. A virgin segment was defined as the segment of a buoy trajectory from 20-35 days at sea, so that the associated FAD likely represents a new deployment which has been potentially colonized by tuna and not already fished.

In this analysis we have obtained from the acoustic signal of the echosounder buoys associated to FADs the biomass of bigeye tuna aggregated under a FAD. The aggregations of bigeye tuna associated with floating objects are mostly composed of small individuals (FL around 48cm). Therefore, the Buoy-derived Abundance Index (BAI) would represent an indicator of BET juvenile; a modal size of 48cm would correspond to around 1 year of life.

Figure 3 shows the histograms of the BAI and log transformed BAI nominal values. Log transformation makes the data to follow a normal distribution, as shown in the left panel of. **Figure 4** shows the spatial distribution [5ºx5º] of the number of "virgin" sequences of buoy trajectories that have been used in the GLM analysis. The quarterly evolution of the number of observations on a 5ºx5º grid is shown in **Figure 5.** The number of observations available has grown considerably over the years, especially since 2013. Only the area between 5ºN and 5ºS and east of 10ºW shows a similar pattern of evolution of the number of observations; the rest of 5ºx5º areas show, in general, non-comparable and more irregular patterns.

Figure *6* shows a table plot of the variables used in the GLM analysis. Independent variables tested in the GLM were year-quarter (yyqq), 5ºx5º area (area), buoy model (model), buoy velocity (vel), FAD density (den), chlorophyll concentration (chl), detected fronts in chlorophyll (chlfront), sea surface temperature (sst), detected fronts in sst (sstfront) and mixed layer height (mid). The dependent variable (BAI) was the 0.9 quantile of the integrated acoustic energy observations in the "virgin" sequence.

Figure 7, Figure 8 and Figure 10 show boxplots of log transformed BAI nominal values for each of the independent variables, expressed as categorical**. Figure 10** shows the quarterly evolution of the log BAI index by squares of 5x5 degrees from 2010 to 2020.

The results of the deviance analysis are shown in **Table 1**. The model explained 41% of the total deviance being the most significant explanatory factors: year-quarter, 5ºx5º area and the interaction year-quarter*area that was considered as random interaction. No significant residual patterns were observed (**Figure 11**).

Quarterly series of standardized BAI index are provided in **Table 2 and Figure 12**. Most of the nominal values are embedded within the confidence interval of the standardized BAI index. The BAI index shows a decreasing trend at the beginning of the series, from 2010 to 2012; then a stabilization period at a low level from 2013 to 2016, followed by an increasing trend in 2017 and 2018 to levels of the beginning of the series, and decrease again in 2019 and 2020. The CVs remain relatively stable (between 11-19%) during the whole time series.

Acknowledgements

This work was supported by the Government of the Basque Country (*Departamento de Desarrollo Económico, Sostenibilidad y Medio Ambiente*) and the EU funded projects RECOLAPE and CECOFAD2. We thank the Spanish vessel owner associations ANABAC and OPAGAC and those companies that have provided acoustic information from their echosounder buoys were: Albacora SA, Atunera Sant Yago SA, Atunsa, Calvopesca El Salvador SA de CV, Cantabrica de Tunidos SAU, Icube Tuna Fisheries NV, Inpesca Fishing Belize Ltd, Integral Fishing Service INC, Intertuna, NV, Overseas Tuna Company NV and Pevasa. We are also thankful to the three buoy providers companies Marine Instruments, Satlink and Zunibal.

References

Bates, D., Mächler, M., Bolker, B., & Walker, S. (2015). Fitting Linear Mixed-Effects Models Using lme4. *Journal of Statistical Software*, *67*(1), 1–48. https://doi.org/10.18637/jss.v067.i01

Belkin, I. M., & O'Reilly, J. E. (2009). An algorithm for oceanic front detection in chlorophyll and SST satellite imagery. *Journal of Marine Systems*, *78*, 319–326. https://doi.org/10.1016/j.jmarsys.2008.11.018

Boyra, G., Moreno, G., Sobradillo, B., Pe, I., Sancristobal, I., & Demer, D. A. (2018). Target strength of skipjack tuna (Katsuwanus pelamis) associated with fish aggregating devices (FADs). *ICES Journal of Marine Science*, *75*, 1790–1802. https://doi.org/10.1093/icesjms/fsy041

Brill, R. V., Block, B. A., Boggs, C. H., Bigelow, K., Freund, E. V., & Marcinek, D. J. (1999). Horizontal movements and depth distribution of large adult yellowfin tuna (Thunnus albacares) near the Hawaiian Islands , recorded using ultrasonic telemetry : implications for the physiological ecology of pelagic fishes. *Marine Biology*, *133*, 395–408.

Dagorn, L., Holland, K., Puente, E., Taquet, M., Ramos, A., Brault, P., … Aumeeruddy, R. (2006). *FADIO (Fish Aggregating Devices as Instrumented Observatories of pelagic ecosystems): a European Union funded project on development of new observational instruments and the behavior of fish around drifting FADs* (No. IOTC-2006-WPTT-16).

Foote, K. G. (1983). Linearity of fisheries acoustics, with addition theorems. *The Journal of the Acoustical Society of America*, *73*(6), 1932–1940. https://doi.org/10.1121/1.389583

Gaertner, D, Ariz, J., Bez, N., Clermidy, S., Moreno, G., Murua, H., & Soto, M. (2016). Objectives and first results of the CECOFAD project. *Collect. Vol. Sci. Pap. ICCAT*, *72*(2), 391–405.

Gaertner, Daniel, Ariz, J., Bez, N., Clermidy, S., Moreno, G., Murua, H., … Marsac, F. (2016). *Results achieved within the framework of the EU research project: Catch, Effort, and eCOsystem impacts of FAD-fishing (CECOFAD)* (No. IOTC-2016-WPTT18-35).

Hampton, I. (1996). Acoustic and egg-production estimates of South African anchovy biomass over a decade: comparisons, accuracy, and utility. *ICES Journal of Marine Science*, *53*(2), 493–500. https://doi.org/10.1006/jmsc.1996.0071

Hoyle, S. D., Huang, J. H., Kim, D. N., Lee3, M. K., Matsumoto, T., & III, J. W. (2019). Standardization of bigeye tuna CPUE in the Atlantic Ocean by the Japanese longline fishery which includes cluster analysis. *Collect. Vol. Sci. Pap. ICCAT*, *75*(7), 2098–2116.

ICES. (2015). *Manual for International Pelagic Surveys (IPS)*. Copenhagen.

Josse, E., Bach, P., & Dagorn, L. (1998). Simultaneous observations of tuna movements and their prey by sonic tracking and acoustic surveys. In *Advances in Invertebrates and Fish Telemetry* (pp. 61–69). https://doi.org/10.1007/978-94-011-5090-3_8

Lo, N. C., Jacobson, L. D., & Squire, J. L. (1992). Indices of Relative Abundance from Fish Spotter Data based on Delta-Lognornial Models. *Canadian Journal of Fisheries and Aquatic Sciences*, *49*(12), 2515–2526.

Lopez, J., Moreno, G., Ibaibarriaga, L., & Dagorn, L. (2017). Diel behaviour of tuna and non-tuna species at drifting fish aggregating devices (DFADs) in the Western Indian Ocean, determined by fishers' echo-sounder buoys. *Marine Biology*, *164*(3), 44. https://doi.org/10.1007/s00227-017-3075-3

Lopez, J., Moreno, G., Sancristobal, I., & Murua, J. (2014). Evolution and current state of the technology of echo-sounder buoys used by Spanish tropical tuna purse seiners in the Atlantic , Indian and Pacific Oceans. *Fisheries Research*, *155*, 127–137. https://doi.org/10.1016/j.fishres.2014.02.033

Maclennan, D., Fernandes, P. G., & Dalen, J. (2002). A consistent approach to definitions and symbols in fisheries acoustics. *ICES Journal of Marine Science*, *59*(2), 365–369. https://doi.org/10.1006/jmsc.2001.1158

Massé, J., Uriarte, A., Angélico, M. M., & Carrera, P. (2018). *Pelagic survey series for sardine and anchovy in ICES subareas 8 and 9 – Towards an ecosystem approach.*

Maunder, M. N., & Punt, A. E. (2004). Standardizing catch and effort data: a review of recent approaches. *Fisheries Research*, *70*(2–3), 141–159. https://doi.org/10.1016/j.fishres.2004.08.002

Maunder, M. N., Sibert, J., Fonteneau, A., Hampton, J., Kleiber, P., & Harley, S. J. (2006). Interpreting catch per unit effort data to assess the status of individual stocks and communities. *ICES Journal of Marine Science*, *63*(8), 1373–1385. https://doi.org/10.1016/j.icesjms.2006.05.008

Methot, R. D., & Wetzel, C. R. (2012). Stock synthesis: A biological and statistical framework for fish stock assessment and fishery management. *Fisheries Research*. https://doi.org/10.1016/j.fishres.2012.10.012

Moreno, G., Boyra, G., Sancristobal, I., & Restrepo, V. (2019). Towards acoustic discrimination of tropical tunas associated with Fish Aggregating Devices. *PloS ONE*, *14*(6), 24. https://doi.org/https://doi.org/10.1371/journal.pone.0216353

Moreno, Gala, Dagorn, L., Sancho, G., & Itano, D. (2007). Fish behaviour from fishers' knowledge: the case study of tropical tuna around drifting fish aggregating devices (DFADs). *Canadian Journal of Fisheries and Aquatic Sciences*, *64*(11), 1517–1528. https://doi.org/10.1139/f07-113

Orue, B., Lopez, J., Moreno, G., Santiago, J., Soto, M., & Murua, H. (2019). Aggregation process of drifting fish aggregating devices (DFADs) in the Western Indian Ocean: Who arrives first, tuna or non-tuna species? *Plos One*, *14*(1), e0210435. https://doi.org/10.1371/journal.pone.0210435

Oshima, T. (2008). *Target strength of Bigeye, Yellowfin and Skipjack measured by split beam echo sounder in a cage.* Indian Ocean Tuna Commission Working Party on Tropical Tunas. (No. WPTT-22).

Punt, A. E., Walker, T. I., Taylor, B. L., & Pribac, F. (2000). Standardization of catch and effort data in a spatially-structured shark fishery. *Fisheries Research*, *45*(2), 129–145. https://doi.org/10.1016/S0165-7836(99)00106-X

Quinn, T. J., & Deriso, R. B. (Richard B. (1999). *Quantitative fish dynamics*. Retrieved from https://books.google.es/books/about/Quantitative_Fish_Dynamics.html?id=5FVBj8jnh6sC&redir_esc=y

Robert, M., Dagorn, L., Lopez, J., Moreno, G., & Deneubourg, J.-L. (2013). Does social behavior influence the dynamics of aggregations formed by tropical tunas around floating objects? An experimental approach. *Journal of Experimental …*, *440*, 238–243. Retrieved from http://www.sciencedirect.com/science/article/pii/S0022098113000099

Røttingen, I. (1976). On the relation between echo intensity and fish density. *FiskDir. Skr. Ser. Havunders.*, *16*(9), 301–314. Retrieved from https://brage.bibsys.no/xmlui/handle/11250/114400

Santiago, J., Lopez, J., Moreno, G., Murua, H., Quincoces, I., & Soto, M. (2016). Towards a tropical tuna buoy-derived abundance index (TT-BAI). *Collect. Vol. Sci. Pap. ICCAT*, *72*(3), 714–724.

Santiago J, Uranga J, Quincoces I, Orue B, Grande M, Murua H, Merino G, Urtizberea A, Zudaire, I, Boyra G. (2019). A Novel Index of Abundance of Juvenile Yellowfin Tuna in the Indian Ocean Derived from Echosounder Buoys. IOTC–2019–WPTT21–47

Santiago J, Uranga J, Quincoces I, Orue B, Grande M, Murua H, Merino G, Urtizberea A, Zudaire, I, Boyra G. (2020a). A Novel Index of Abundance of Skipjack in the Indian Ocean Derived from Echosounder Buoys. IOTC-2020-WPTT20-14

Santiago J, Uranga J, Quincoces I, Orue B, Grande M, Murua H, Merino G, Urtizberea A, Pascual P, Boyra G. (2020b). A Novel Index of Abundance of Juvenile Yellowfin Tuna in the Atlantic Ocean Derived from Echosounder Buoys. Collect. Vol. Sci. Pap. ICCAT, 76(6): 321-343

Scott, G. P., & Lopez, J. (2014). *The use of FADs in Tuna Fisheries*. European Parliament. Policy Department B: Structural and Cohesion Policies: Fisheries. IP/B/PECH/IC/2013.

Simmonds, E. J., & MacLennan, D. N. (2005). *Fisheries acoustics : theory and practice*. Blackwell Science.

Torres-Irineo, E., Gaertner, D., Chassot, E., & Dreyfus-León, M. (2014). Changes in fishing power and fishing strategies driven by new technologies: The case of tropical tuna purse seiners in the eastern Atlantic Ocean. *Fisheries Research*, *155*, 10–19. https://doi.org/10.1016/j.fishres.2014.02.017

Table 1. Deviance table for the GLM lognormal model of the 2010-2020 period. Significant (p<0.05) factors and interactions explaining >5% of total deviance are highlighted.

Variable	Df	Deviance	Resid..Df	Resid..Dev	F	Pr..F.	Dev..Exp
NULL	NA	NA	33612	48586	NA	NA	NA
yyqq	43	4816	33569	43770	129	0	9.91%
area	31	8574	33538	35196	319	0	17.65%
model	1	813	33537	34383	937	0	1.67%
den	1	64	33536	34320	73	0	0.13%
chl	1	74	33535	34246	85	0	0.15%
chlfront	1	41	33534	34205	47	0	0.08%
sst	1	30	33533	34175	35	0	0.06%
sstfront	1	2	33532	34173	2	0.1557	0%
mld	1	68	33531	34105	79	0	0.14%
yyqq:area	1247	5530	32284	28575	5	0	11.38%
yyqq:model	26	140	32258	28434	6	0	0.29%
yyqq:den	43	338	32215	28096	9	0	0.70%
yyqq:sst	43	151	32172	27945	4	0	0.31%
yyqq:mld	43	69	32129	27876	2	0.0007	0.14%

Table 2. Nominal and standardized Buoy-derived Abundance Index for the period 2010-2020. Standard errors and coefficient of variations of the standardized series are also included.

Quarter	Index nominal	BAI Index	BAI se	BAI cv	Quarter	Index nominal	BAI Index	BAI se	BAI cv
10Q1	0.325	0.357	0.065	0.182	**15Q3**	0.218	0.207	0.023	0.11
10Q2	0.29	0.231	0.041	0.177	**15Q4**	0.198	0.199	0.019	0.096
10Q3	0.332	0.266	0.049	0.184	**16Q1**	0.153	0.168	0.02	0.12
10Q4	0.465	0.434	0.077	0.178	**16Q2**	0.103	0.132	0.021	0.158
11Q1	0.311	0.32	0.061	0.192	**16Q3**	0.165	0.216	0.028	0.129
11Q2	0.234	0.215	0.039	0.182	**16Q4**	0.207	0.2	0.022	0.111
11Q3	0.182	0.162	0.029	0.181	**17Q1**	0.144	0.172	0.022	0.13
11Q4	0.258	0.183	0.034	0.184	**17Q2**	0.196	0.189	0.027	0.144
12Q1	0.166	0.154	0.029	0.185	**17Q3**	0.224	0.261	0.036	0.137
12Q2	0.158	0.153	0.027	0.179	**17Q4**	0.301	0.319	0.035	0.111
12Q3	0.149	0.143	0.026	0.178	**18Q1**	0.285	0.324	0.041	0.127
12Q4	0.128	0.132	0.023	0.177	**18Q2**	0.305	0.343	0.049	0.144
13Q1	0.125	0.146	0.026	0.176	**18Q3**	0.312	0.384	0.05	0.131
13Q2	0.083	0.114	0.018	0.16	**18Q4**	0.391	0.355	0.045	0.125
13Q3	0.117	0.13	0.019	0.144	**19Q1**	0.34	0.405	0.061	0.149
13Q4	0.19	0.218	0.03	0.137	**19Q2**	0.281	0.281	0.044	0.156
14Q1	0.154	0.191	0.028	0.147	**19Q3**	0.263	0.352	0.056	0.159
14Q2	0.097	0.118	0.017	0.143	**19Q4**	0.361	0.342	0.052	0.151
14Q3	0.151	0.194	0.024	0.126	**20Q1**	0.211	0.195	0.029	0.147
14Q4	0.18	0.197	0.023	0.117	**20Q2**	0.166	0.209	0.033	0.156
15Q1	0.16	0.178	0.023	0.13	**20Q3**	0.133	0.169	0.027	0.16
15Q2	0.121	0.12	0.016	0.135	**20Q4**	0.271	0.283	0.044	0.154

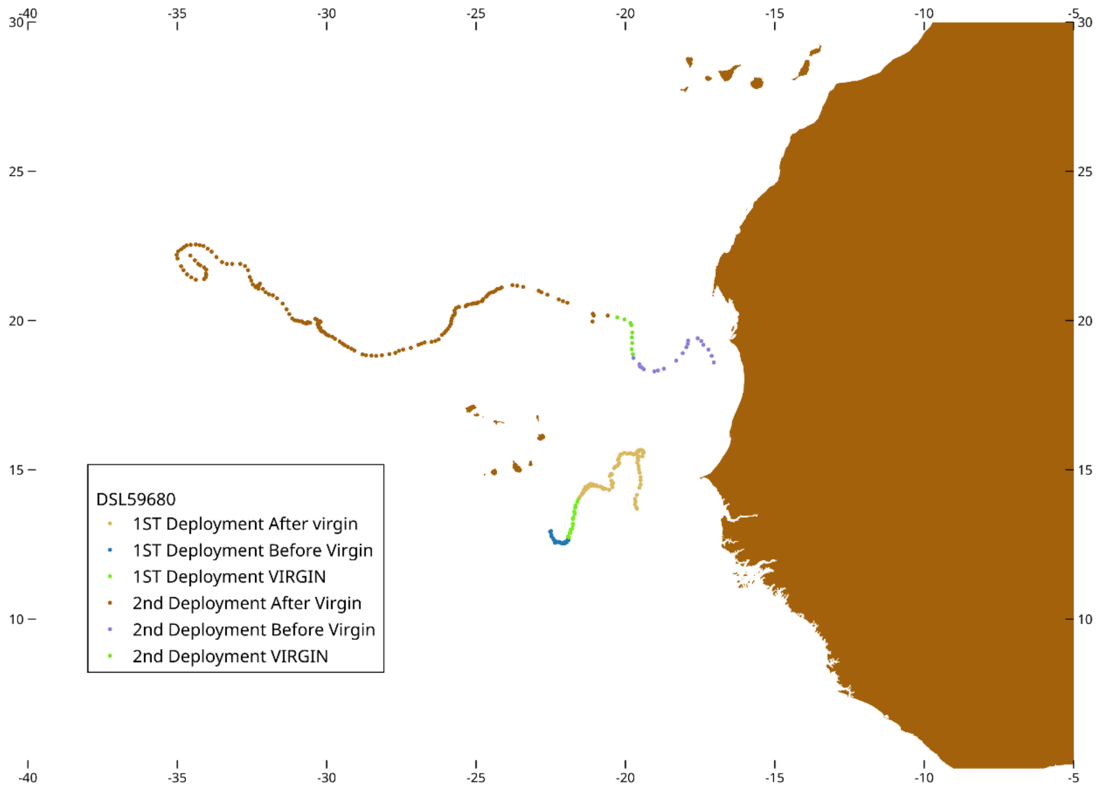

Figure 1. Example of "virgin" segments used for the calculation of the BAI index. Trajectories correspond to buoy DSL59680 with two different paths representing drifts of different FADs. A virgin segment is defined as the segment of a buoy trajectory whose associated FAD likely represents a new deployment, which has been potentially colonized by tuna and not already fished. We consider as virgin segments (i.e. when tuna has aggregated to FAD) those segments of trajectories from 20-35 days at sea. "Virgin" segments are shown in green in the Figure.

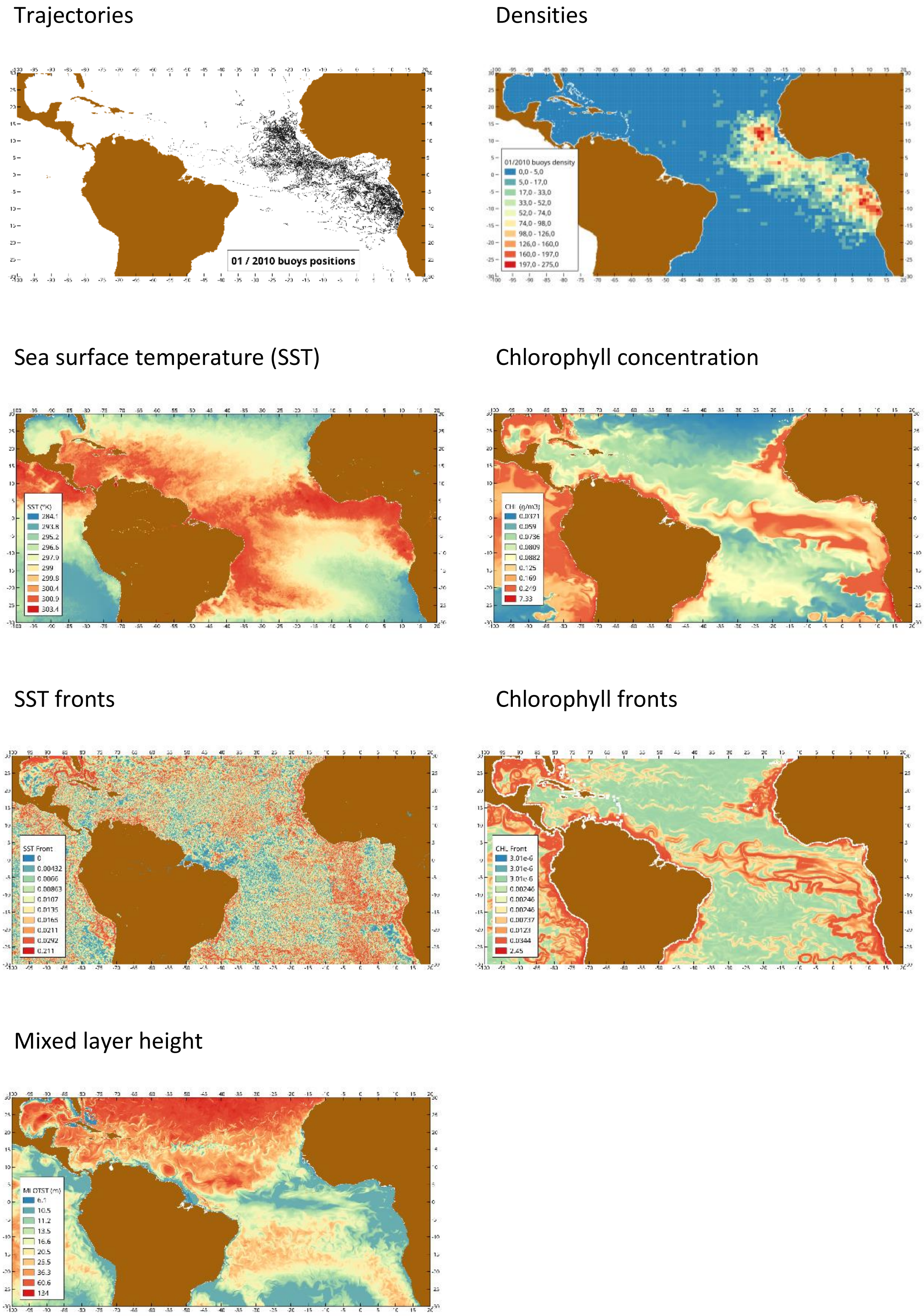

Figure 2. Example of one month of data, January 2010, of buoy trajectories, density of buoys by 1ºx1º and environmental variables incorporated in the GLM analysis: sea surface temperature (SST), chlorophyll concentration, detected fronts in SST, detected fronts in chlorophyll and mixed layer height.

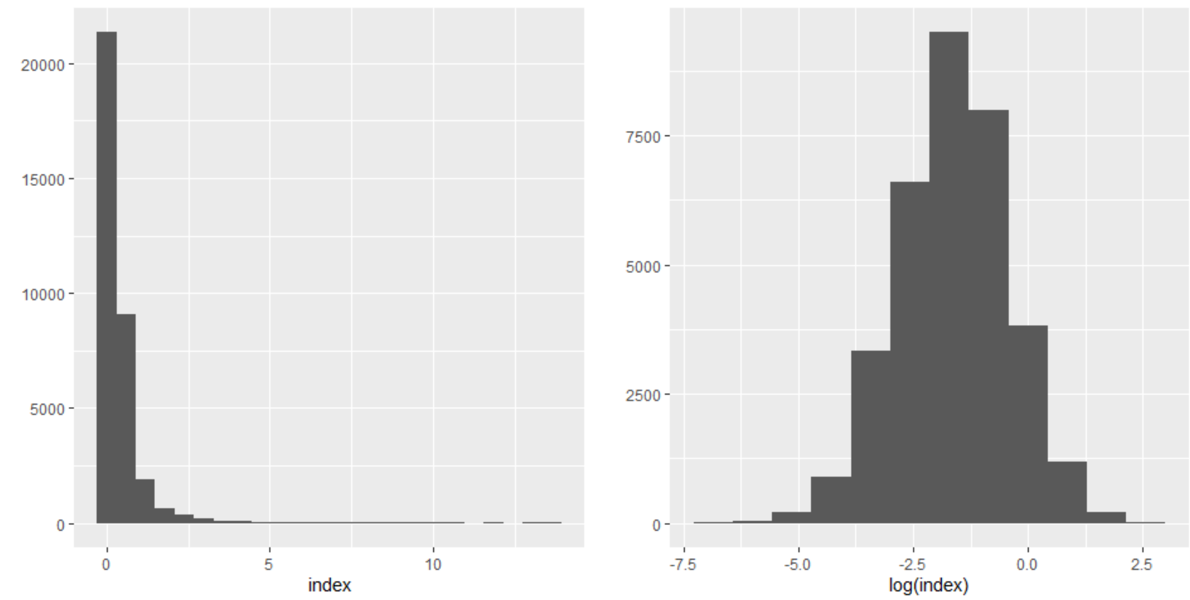

Figure 3. Histograms of the nominal values (left) and the log transformed nominal values (right) of the Buoy-derived Abundance Index (0.9 quantile of the integrated acoustic energy observations in "virgin" sequences).

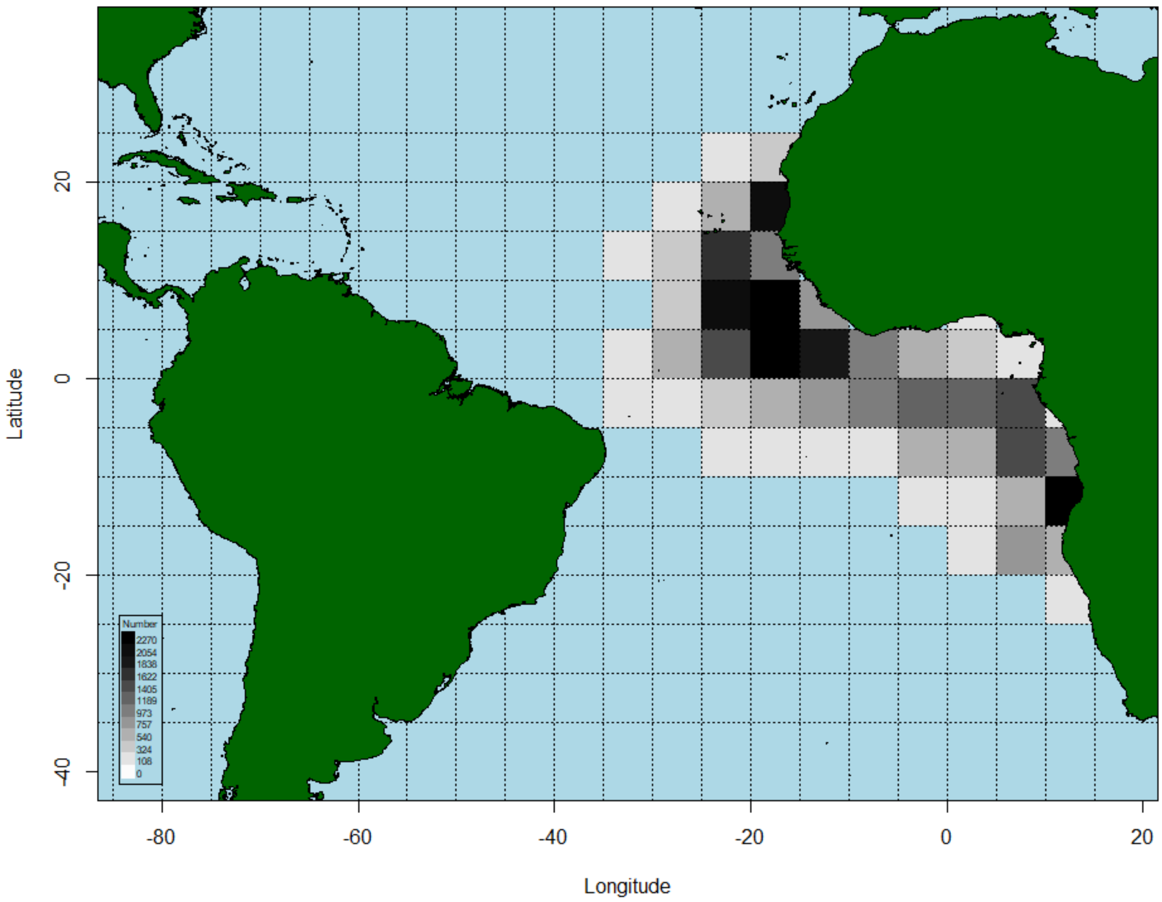

Figure 4. Spatial distribution [5ºx5º] of the "virgin" sequences of buoy trajectories that have been used in the GLM analysis.

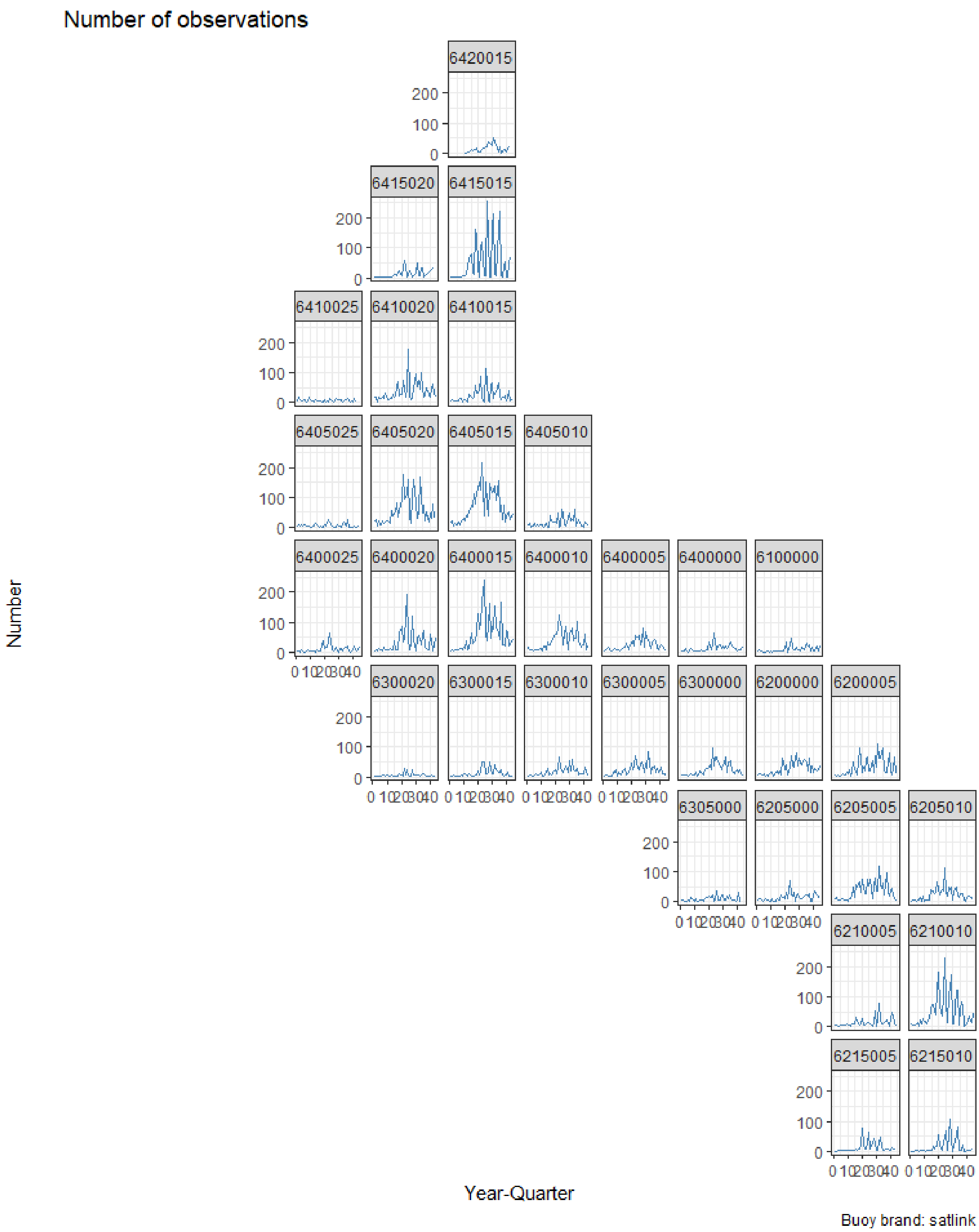

Figure 5. Quarterly evolution of the number of observations ("virgin" sequences of buoy trajectories) on a 5ºx5º grid.

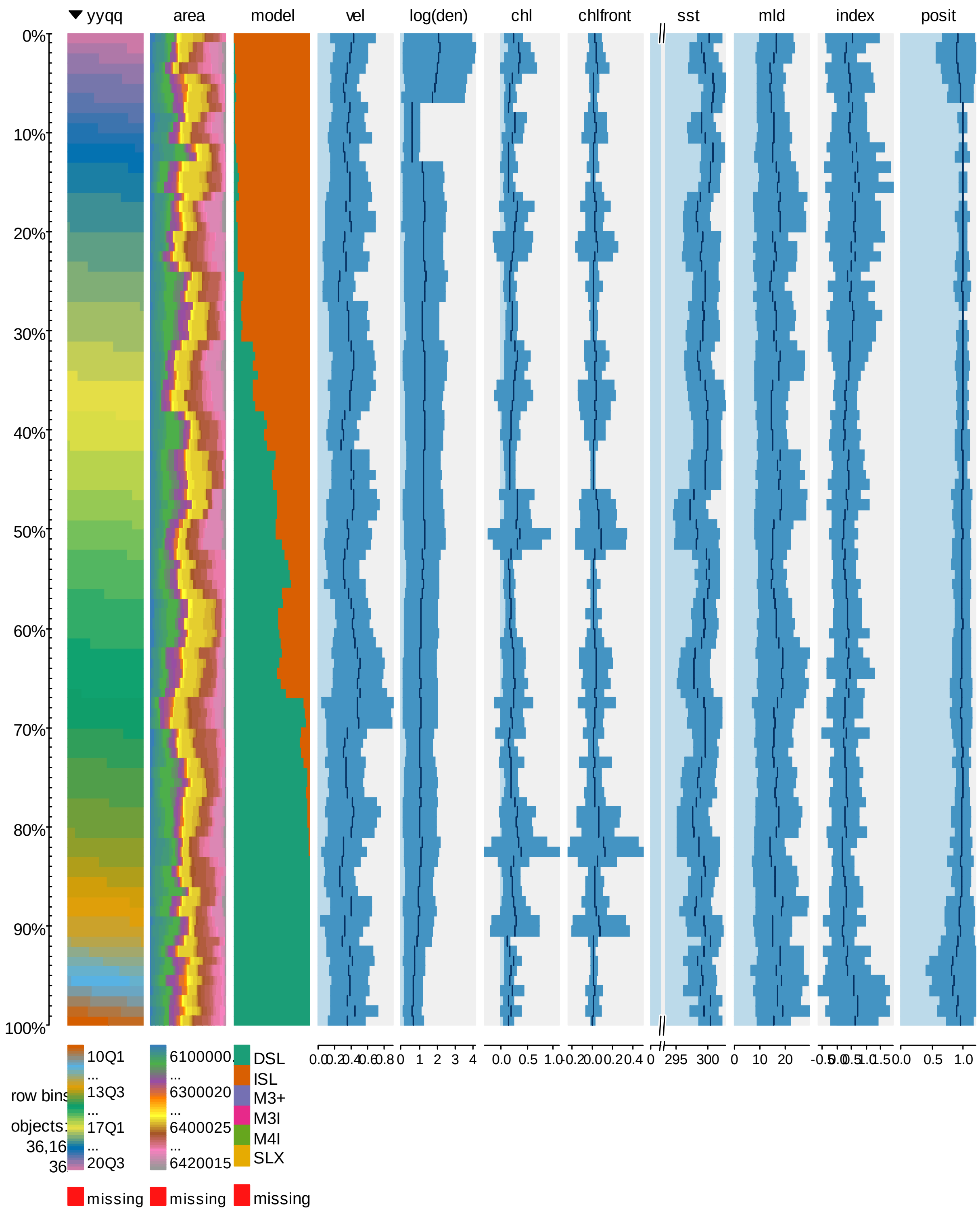

Figure 6. Tableplot of the variables used in the GLM analysis. Each column represents a variable and each row bin is an aggregate of a certain number of records. For numeric variables, a bar chart of the mean values is depicted. For categorical variables, a stacked bar chart is depicted of the proportions of categories. Independent variables tested in the GLM were year-quarter (yyqq), 5ºx5º area (area), buoy model (model), buoy velocity (vel), FAD density (den), chlorophyll concentration (chl), detected fronts in chlorophyll (chlfront), sea surface temperature (SST), detected fronts in SST (sstfront) and mixed layer height (mid). The dependent variable for the lognormal component was the 0.9 quantile of the integrated acoustic energy observations in the "virgin" sequence (index); and for the binomial component, the proportion of positives (posit).

A) Year-quarter

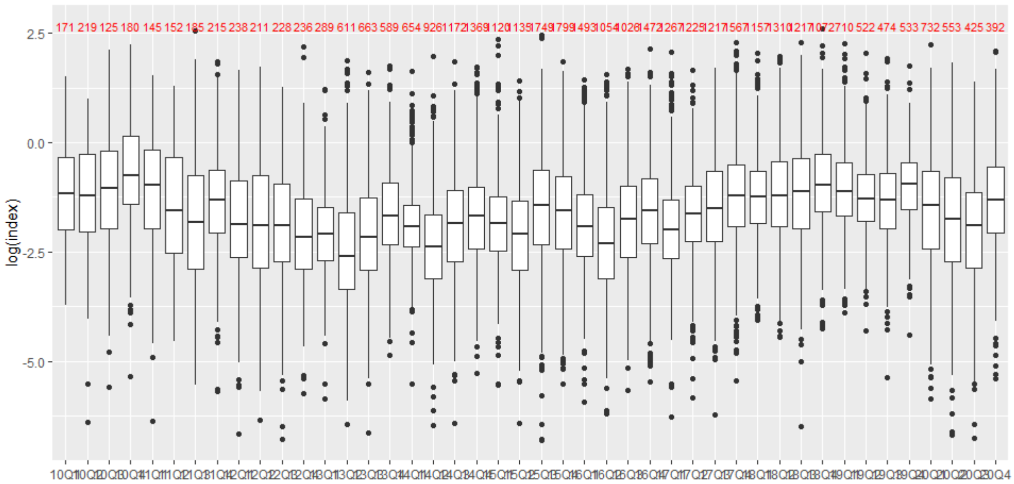

B) Buoy model

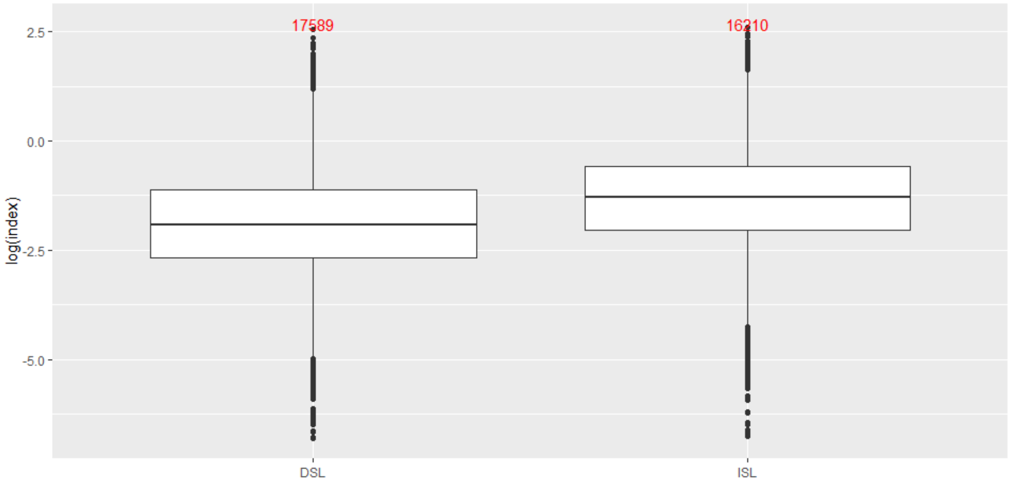

C) Buoy speed

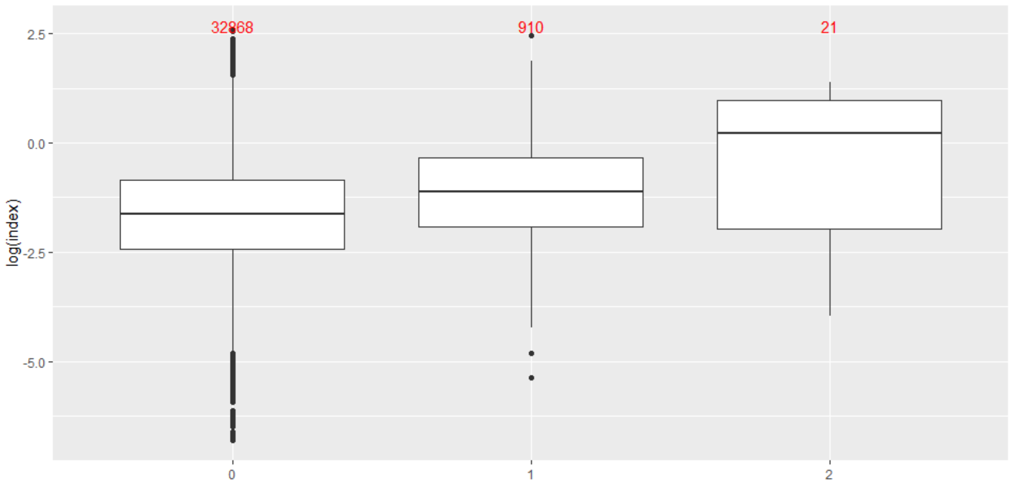

Figure 7. Boxplot of log (BAI) for year-quarter, buoy model and buoy speed (expressed as categorical). Number of observations for each categorical value is shown in red.

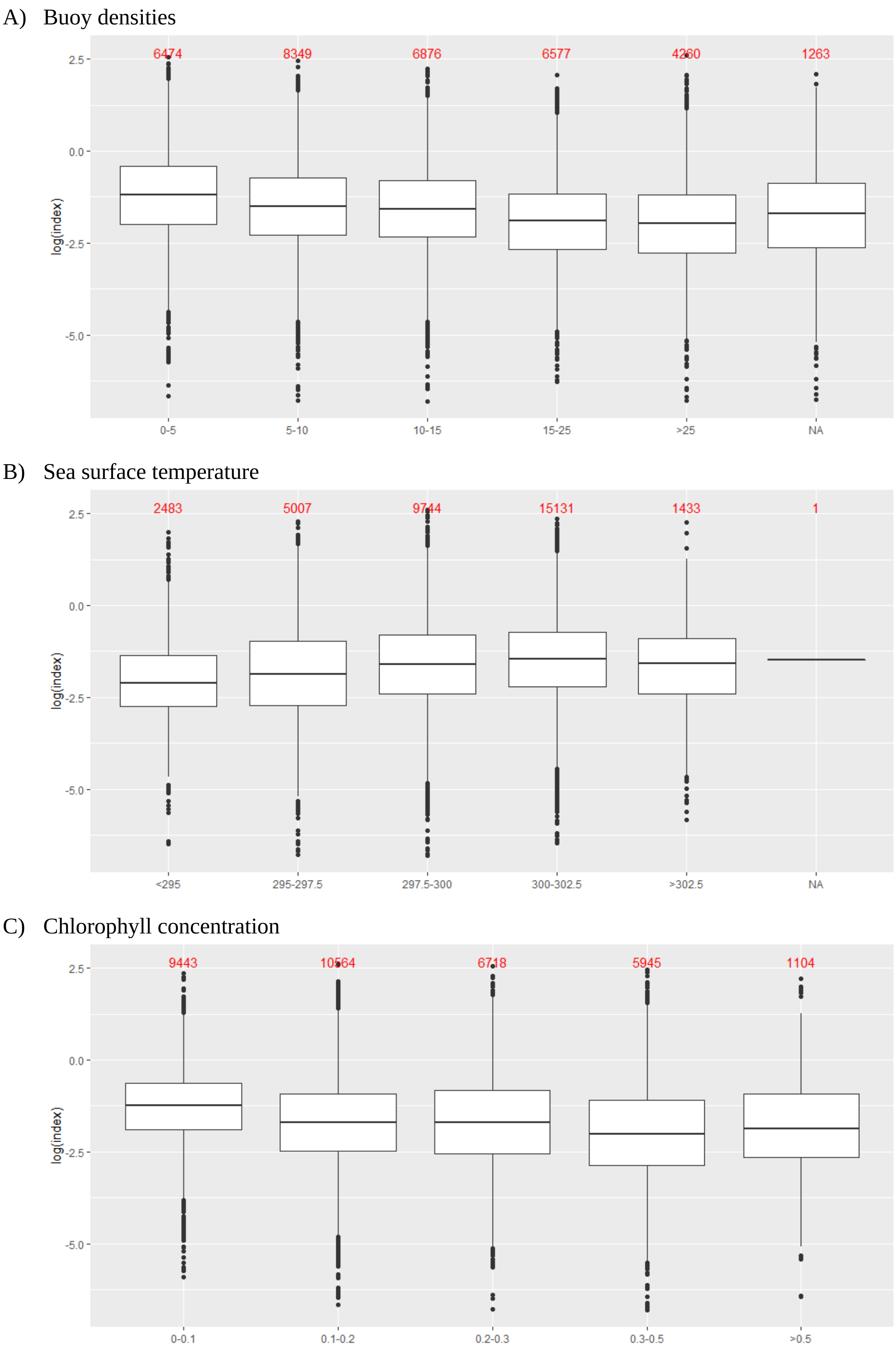

Figure 8. Boxplot of log (BAI) for buoy densities, sea surface temperature and chlorophyll concentration (expressed as categorical). Number of observations for each categorical value is shown in red.

A) Fronts of sea surface temperature

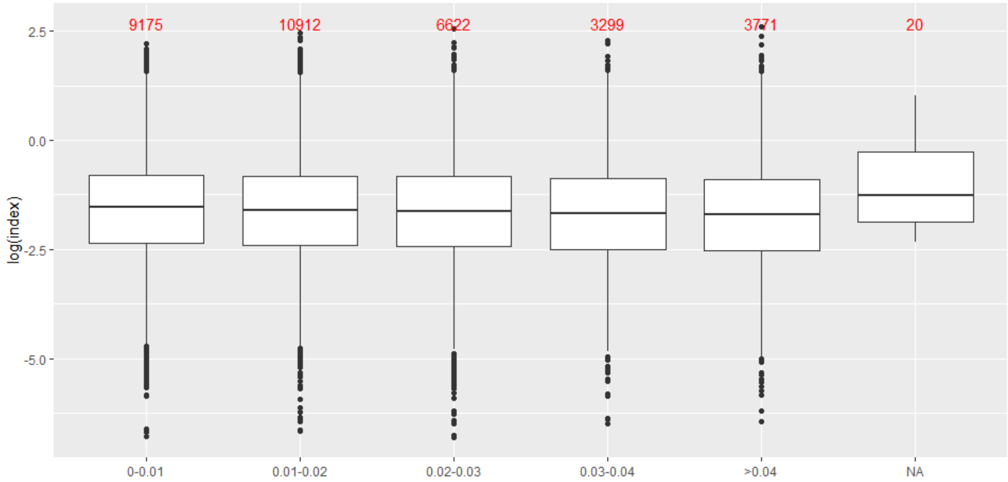

B) Fronts of chlorophyll concentration

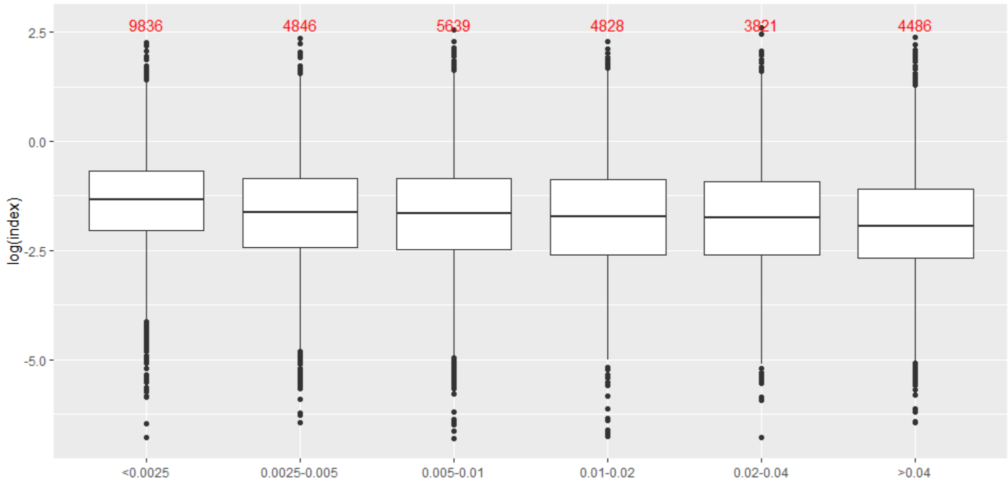

C) Mixed layer height

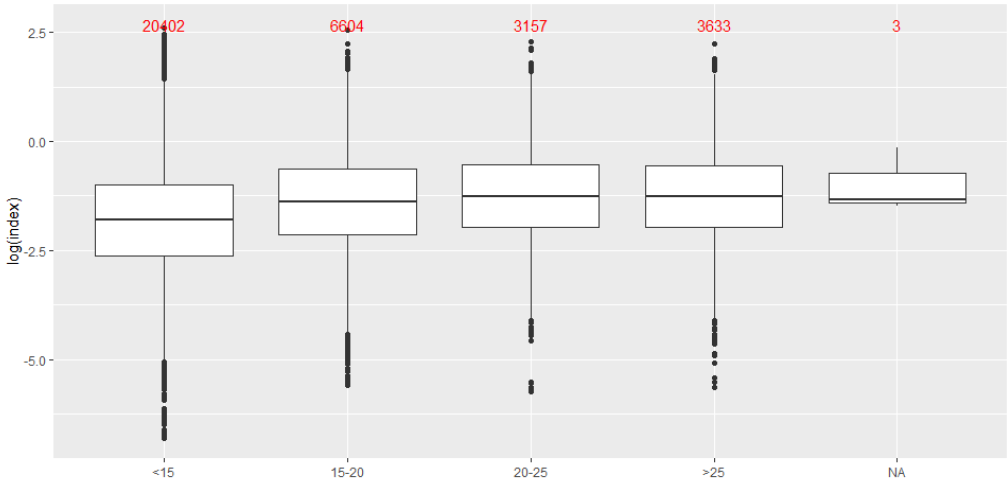

Figure 9. Boxplot of log (BAI) for fronts of sea surface temperature, fronts of chlorophyll concentration and mixed layer height (expressed as categorical). Number of observations for each categorical value is shown in red.

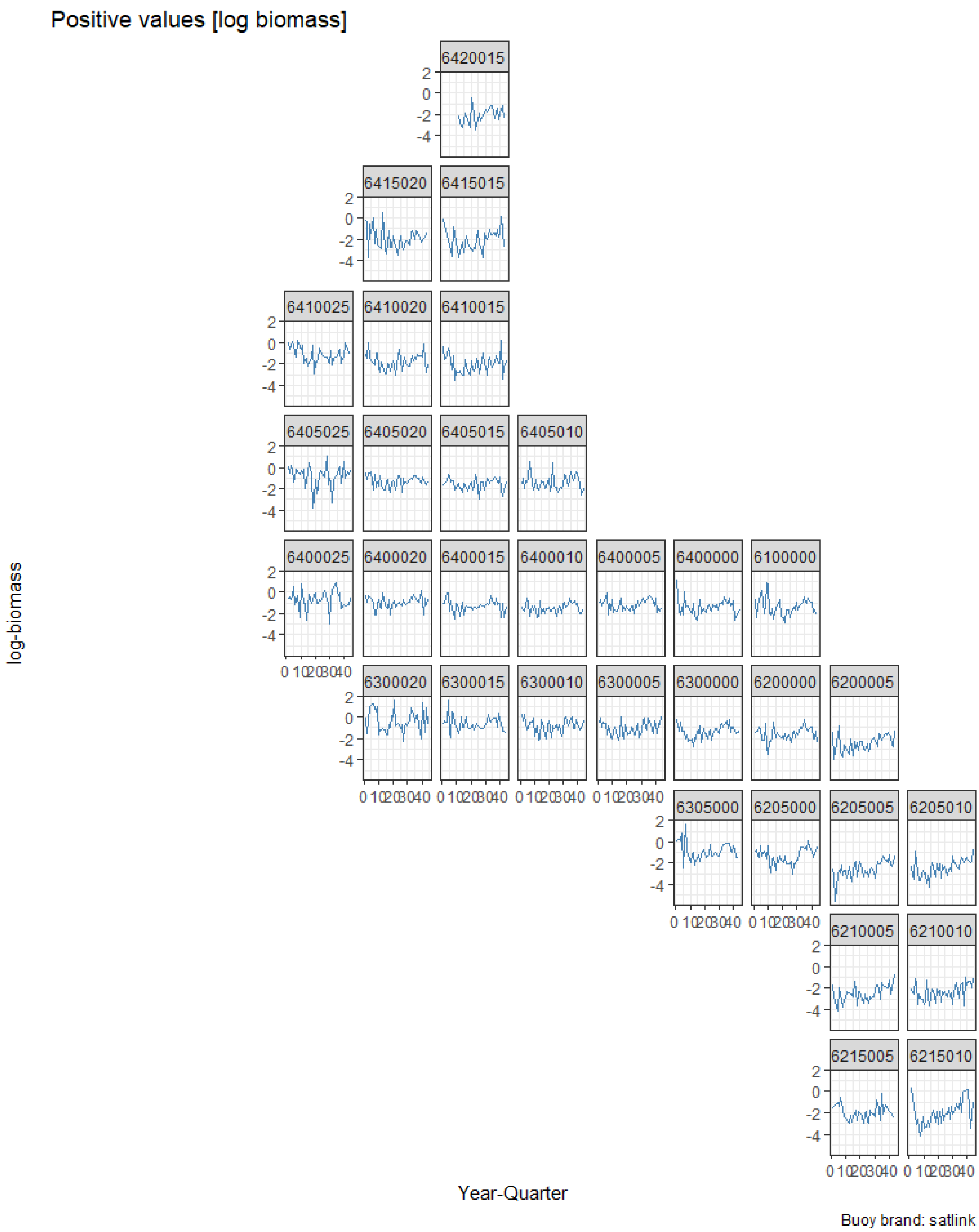

Figure 10. Quarterly evolution of the log BAI index in the Atlantic Ocean by squares of 5x5 degrees from 2010 to 2020.

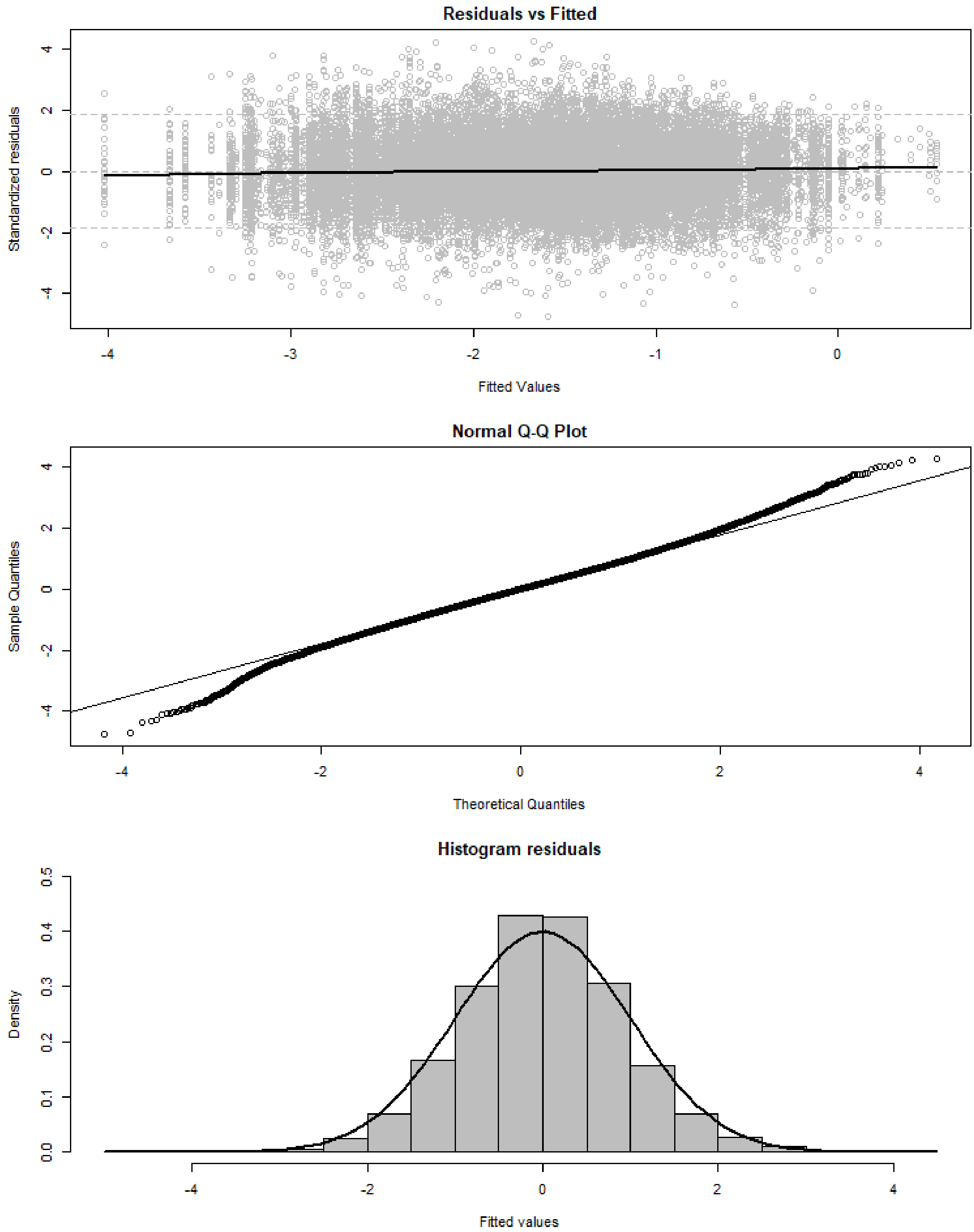

Figure 11. Diagnostics of the lognormal model selected for the period 2010-2020: residuals vs fitted, Normal Q-Q plot and frequency distributions of the residuals.

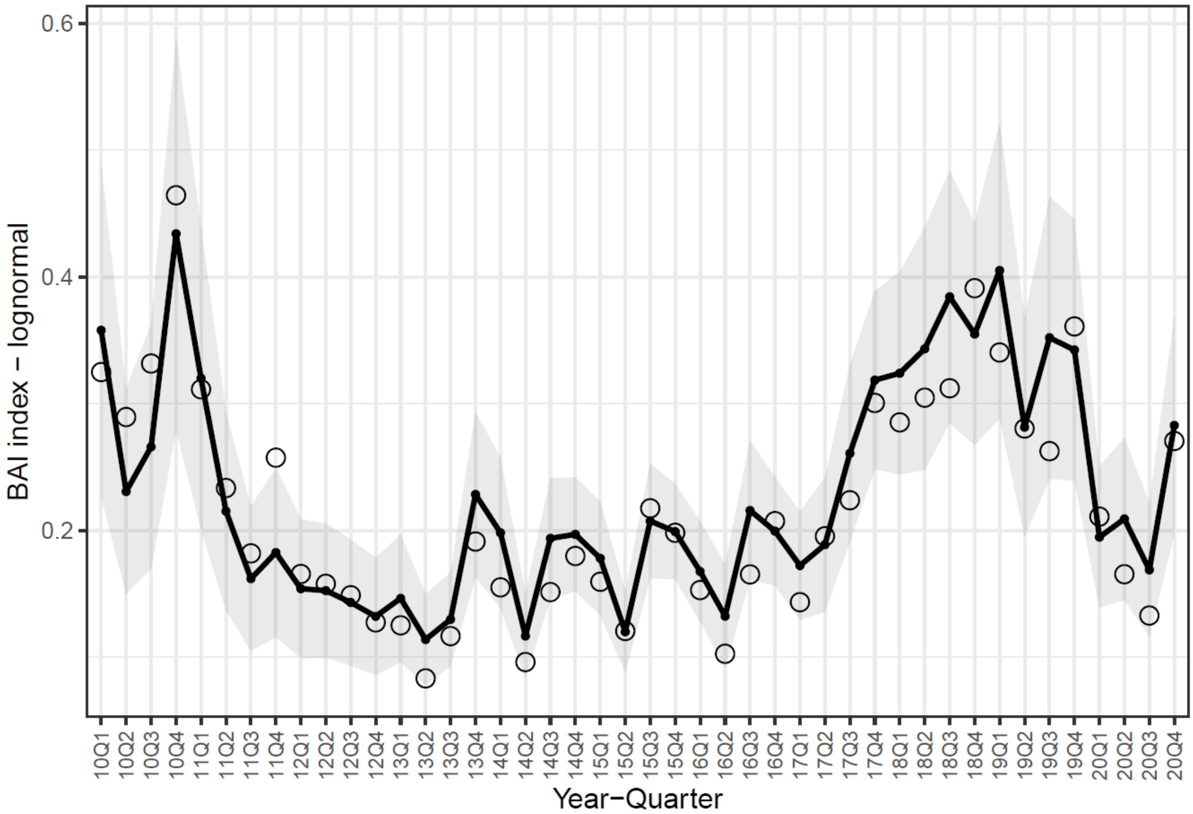

Figure 12. Time series of nominal (circles) and standardized (continuous line) Buoy-derived Abundance Index for the period 2010-2020. The 95% upper and lower confidence intervals of the standardized BAI index are shown.